SAND2019-8906C

Multi-Layered Solid State Neutron Sensor

W.C. Rice, J.E. Levy, D.P. Adams, D.R. Nichols, R.K. Harrison, M. Jordan,
A. Jones, L.D. Claus, S.E. Jensen, D.J. Dorsey and R. Koudelka
Sandia National Laboratories, Albuquerque, NM, email: wcrice@sandia.gov

***Abstract*—**A solid state neutron sensor was developed which makes use of the boron-10 (n, alpha) reaction to convert incident thermal neutrons into detectable electronic signals. The ^{10}B reaction offers unique advantages for a small detector because the reaction products have high energies which can generate, by impact ionization, a large number of carriers in semiconductor materials. The sensor is made as a stack consisting of multiple layers alternating between converter material (boron) and collector semiconductor material (silicon). As the number of these bi-layers increases, the probability of a neutron interacting with at least one of the layers – so it is captured in the detector before it has a chance to pass through – approaches unity. As a result, the sensor can be made very thin while also remaining highly efficient. Calculations have shown that a multi-layer sensor with an efficiency greater than 70% is feasible. A prototype device of five layers was built with 20% detection efficiency for incident thermal neutrons within an active thickness of 100 microns over a square cm area.

I. Introduction

Neutron detection is critical in nonproliferation applications associated with the identification of special nuclear materials. Gas filled proportional counters using helium-3 (He-3), typically with efficiencies of 17%, have been the most ubiquitous neutron detectors for decades, but they have drawbacks associated with their large size and high voltage requirements. Existing solid-state neutron sensor designs utilizing high neutron cross-section materials have low detection efficiency relative to He-3 sensors due to the challenge of "collecting" charge generated by neutron capture reaction products in high-density converter materials [1].

To increase neutron detection efficiency, relative to other ^{10}B research reported in the literature, our sensor design maximizes the competing optimizations for neutron absorption rate and reaction product collection rate. This is achieved by the stack made of multiple layers. Designs attempting to maximize the collection volume relative to the absorption have been reported in the literature [2,3]. Instead of vertical stacking, these designs have used grooves etched into the silicon collector to maximize collection surrounding a single boron layer while also overcoming the challenge of getting the boron to adhere to the silicon [4]. Significant boosts to efficiencies have been achieved, with these designs reaching as high as 40%.

II. Details of the Design

A. Principles of Operation

Boron is uniquely suited as a converter material for interaction with thermal neutrons because its atomic size is ideal for neutron interaction collisions (Z=5), giving it a relatively high reaction cross section of 3890 barns. Furthermore, when neutrons do collide with boron-10, it produces these high-energy reaction products [4]:

94% of the time:
$^{10}B + n \rightarrow$ $^{7}Li(840keV) + \alpha(1.47MeV) + \gamma(480keV)$,
Q = 2.310 MeV (1st excited state)
6% of the time:
$^{10}B + n \rightarrow$ $^{7}Li(1.015MeV) + \alpha(1.78MeV)$,
Q = 2.792 MeV (to ground state)

Both reactions produce a high energy lithium atom and a high energy alpha particle which are capable of penetrating into silicon or other semiconductor materials to produce electron-hole pairs (1 electron-hole pair is created for every 3.6eV in silicon) by impact ionization. These charge carriers can then be collected electronically by a substrate which essentially is acting as a photodiode. A 1.47MeV alpha particle will penetrate to an average depth of 5.15 microns and generate 400,000 electron-hole pairs provided it enters directly into silicon at normal incidence (see Figures 1 and 2). So once the particles enter the collection volume of semiconductor material, enough electron hole pairs are generated which can be harvested via electrodes to produce an electronic signal (see Figures 3 and 4).

B. Prototype

To produce a working prototype, we made use of existing photodiode material that was built for a photodiode array device in the Silicon Fab at Sandia National Laboratories. This material was made from specialty float zone SOI (silicon on insulator) wafers which were used as starting material developed by a custom process. This material was oxide bonded to a handle wafer and the float-zone material was thinned to a given thickness of ~25um. Once thinned, the photodiode fabrication took place with the addition of processing implants, contact and a single metal layer.

In order to prevent the reaction products (alpha particle or ^{7}Li) from being absorbed in the overlayers before reaching the active photodiode volume, some of the oxide must be removed. "Pockets" were etched into the oxide for boron deposition. This was accomplished by etching the samples in an inductively coupled plasma (ICP) for a short time and measuring the remaining oxide with a white light interferometer.

The thin films of boron-10 were constructed by first depositing a 25 nm Ti adhesion layer. Immediately afterwards

Sandia National Laboratories is a multimission laboratory managed and operated by National Technology & Engineering Solutions of Sandia, LLC, a wholly owned subsidiary of Honeywell International Inc., for the U.S. Department of Energy's National Nuclear Security Administration under contract DE-NA0003525.

^{10}B was deposited along with Al in a multilayer configuration in order to reduce stress-induced buckling. As shown in Figure 5, boron layers (125 nm) were alternated with Al (20 nm). Altogether, 16 bilayers of B/Al were deposited. As a final step, 50 nm Ti was sputter deposited onto the top of the film. This final Ti cap layer proved useful for preventing oxidation of underlying boron. The Al interlayers proved useful for reducing the residual stress of the deposit. The overall thickness of the film was 2.395 μm. This thickness represents a maximum in the amount of alpha particles that are generated and escape from the film without being absorbed [2].

Film stress was managed to reasonable levels, ~ -300 MPa (compressive, in plane). Residual stress was determined using wafer curvature methods employing Stoney's equation. There was no evidence of stress-induced buckling or tensile cracking immediately after deposition or months later (after storage in air).

III. Measurements

Readout of semiconductor detectors requires a charge-based readout configuration because detector capacitance can vary with readout. This is done using a charge sensitive amplifier (CSA) as a preamplifier as shown in Figure 6. Output voltage amplitude is tied to input signal via the transfer function $Vout \cong -Qin/Cf$ where V_{out} is the output voltage of the CSA, Q_{in} is the input charge, and C_f is the feedback capacitance of the CSA that dictated total amplifier gain.

Pulse shaping the output of a CSA allows for reducing pile up under high fluence applications as well as the possibility to add additional gain to the system and filtering out noise due to the band pass nature of the shaping amplifier.

This work used a Cremat CR-S-1us nth order shaping amplifier with a shaping time of 1 μs and an adjustable voltage gain of 1 to 100. This commercially available system also included the Cremat CR-210 baseline restoration module to correct for undershoot that can occur at high count rates.

Once the detector input signal has been amplified and conditioned to filter out broad band noise elements and provide a large enough signal to process, this signal is input to a Multi-Channel Analyzer or MCA. This is an Analog to Digital Converter (ADC) with results displayed in a plot of ADC bins versus counts. This plot provides an energy spectrum to facilitate particle discrimination.

Radiation testing is typically performed by conducting a "dark" count test where the radiation source is removed and a readout of the detector is recorded for the same amount of time as a live or "hot" test with the sensor under live irradiation with a source present. The experimental set-up for conducting the radation tests is shown in Fig. 7.

IV. Analysis

The results from measurements on the two-layer prototype device (Fig. 8) are shown in Fig. 10. As shown in the Figure, the bottom layer (A), having only its topside coated, had a count rate of 5.05 cps. The top layer (B), having its topside coated and also a window opened below it, had a higher count rate of 5.97 cps. When measuring both layers combined (C), the count rate went up to 9.71 cps. The combined measurement is not the sum of the two channels separately, which would be 11.02 cps. This is due to the increased capacitance, noise and leakage of the combined measurement and indicates a potential need, in a final device assembly where the read-out electronics are on the chip with the sensor, to handle each layer individually, or better yet each optimally sized pixels within each layer, in order to minimize the input leakage/capacitance.

Based on the results shown in Fig. 10, as well as the results for an additional three-layer prototype (Fig. 9) shown in Fig. 11, the best layer of the prototype "as-built" device was capable of detecting 5.97 counts per second above background noise. This result aligns well with calculations performed by Monte Carlo Neutral Particle (MCNP) simulation modeling using the exact structure of the prototype (Fig.12). Using this value, the expected value for maximum efficiency for a 5-layer device, based on the operation of a single layer at 5.97 cps (best observed value) acting together with the 192 uCi Cf-252 source, is approximately 21%, indicating the as-built device is already comparable to helium-3 based detectors. Importantly, when the device is made to 20 layers, efficiency goes to 45.5% and at 40 layers (where all neutrons are captured), efficiency becomes 50.8%.

V. Conclusion

A prototype sensor was developed consisting of a three bi-layer stack of alternating converter material (^{10}B) and collector material (silicon photodiode). The stack was assembled on a custom-configured layer structure ("wedding cake"), having a total sensor volume of a 1 square centimeter area by a 100 micron thick active layer. The prototype exhibited promising "as-built" sensitivity of 5.3% detection of thermal neutrons (i.e. 1 out of 20) for an individual sensor bi-layer while being insensitive to gamma irradiation. A five-layer device has a detection efficiency of approximately 21% and is already competitive with the state-of-the-art.

References

[1] A. N. Caruso (2010), *The physics of solid-state neutron detector materials and geometries*, J. Phys.: Condens. Matter 22.

[2] D.S. McGregor, R.T. Klann, H.K. Gersh, J.D. Sanders (2001), *Design considerations for thin-film-coated semiconductor thermal neutron detectors –I: Basics for alpha particle emitting neutron reactive films*, Nuclear Science Symposium Conference Records, IEEE, Vol 4.

[3] R.G. Fronk, S.L.Bellinger, L.C.Henson, D.E.Huddleston, T.R.Ochs, T.J.Sobering, D.S.McGregor, "*High-efficiency microstructured semiconductor neutron detectors for direct ^{3}He replacement*," Nuclear Instruments and Methods in Physics Research A, 779 (2015) 25–32.

[4] D.S. McGregor, R.T. Klann, H.K. Gersh, E. Ariesanti, J.D. Sanders, "*New Surface Morphology for Low Stress Thin-Film-Coated Thermal Neutron Detectors*," IEEE Trans. on Nucl. Science, vol. 49, 4 (2002).

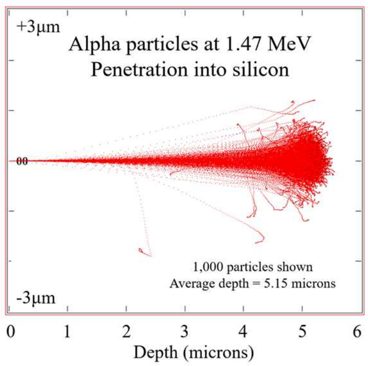

Fig. 1. Penetration of 1.47MeV alpha particles into silicon (SRIM calculation).

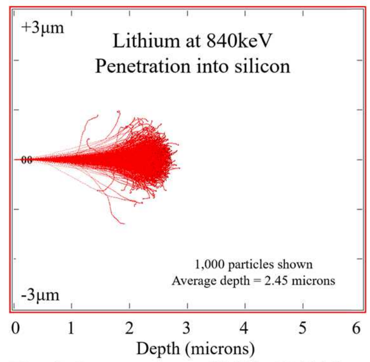

Fig. 2. Penetration of 840keV lithium atoms into silicon (SRIM calculation).

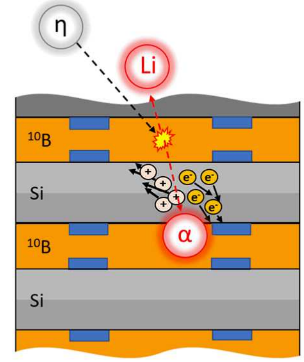

Fig. 3. The multi-layer. Alpha particles and lithium atoms penetrate into collection volumes of silicon on either side of the boron, producing ionized charges which are collected by electrodes (blue) to produce an electronic signal of a strike.

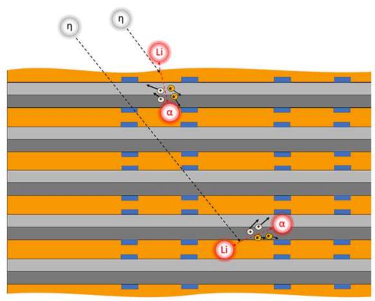

Fig. 4. Multi-layer stack operation. Neutrons not captured in the topmost layers are captured by another boron layer further in.

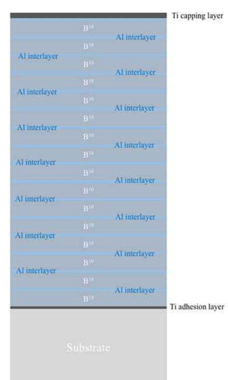

Figure 5. Schematic illustration of boron-containing thin film used for research. Depiction is not to scale but includes all layers.

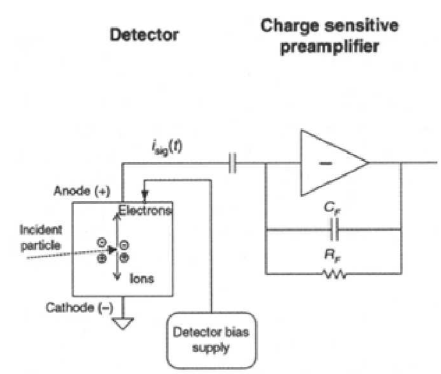

Fig. 6. Schematic of the Charge Sensitive Preamplifier.

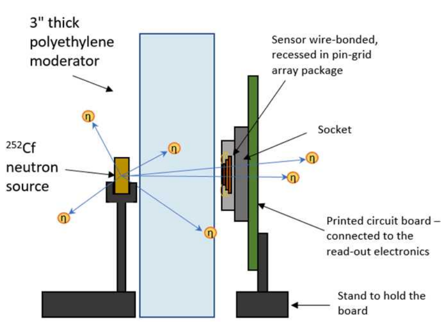

Figure 7. Diagram of the experimental set-up used to conduct measurements with the "wedding cake" prototype.

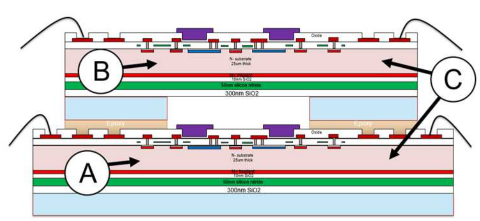

Figure 8. Notional two-layer stack, "wedding cake" for neutron sensing. Not so scale. Boron shown in purple, with both front pocket oxide etches as well as backside silicon etches to decrease material between the boron and detection layers. Circled letters in the diagram shows where signals were collected from for the data shown in Figure 8.

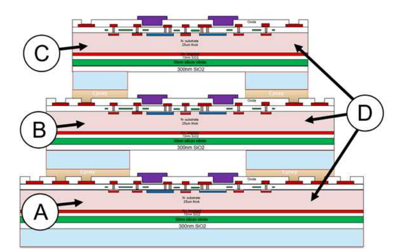

Figure 9. Notional three-layer stack, "wedding cake" for neutron sensing. Not to scale. Boron shown in purple, with both front pocket oxide etches as well as backside silicon etches to decrease material between the boron and detection layers. Circled letters in the diagram shows where signals were collected from for the data shown in Figure 8.

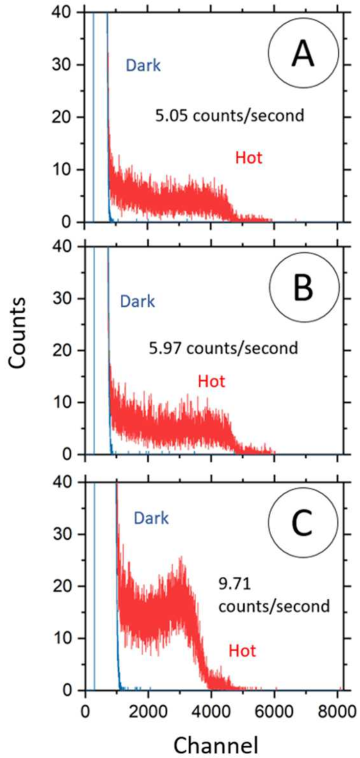

Fig. 10. Results from one-hour measurements of the two-layer stack. Data collected from the two-layer stack, where the top layer has an etch above filled with boron and an etch below it to allow penetration of alphas from the layer below (see Figure 20). Data from (A) bottom layer only, (B) top layer only, and (C) both layers combined. The dark counts (blue curve) are a measure of the background and were collected when the source was not present, whereas the hot counts (red curve) were collected when the source was present. The source was a 192 uCi californium-252 source.As shown in the plot, there is a very clear threshold above which the hot counts (red) can be distinguished from the dark count noise (dark blue – a high number of counts with a steep line going outside of the range of the plot). Dark count "noise" also appears in the results for the hot counts, with the red line overlapping the dark blue line in this region. Channel values are arbitrary units binned by the MCA. They represent voltage spikes that correspond to the total energy of the charge collected in the substrate.

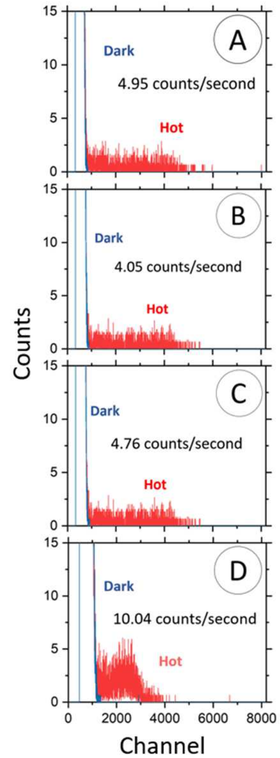

Fig. 11. Results from 6-minute measurements on the three-layer stack with a 192 μCi Cf-252 source. As shown in the plot, there is a very clear threshold above which the hot counts (red) can be distinguished from the dark count noise (dark blue – a high number of counts with a steep line going outside of the range of the plot). Dark count "noise" also appears in the results for the hot counts, with the red line overlapping the dark blue line in this region. Channel values are arbitrary units binned by the MCA. They represent voltage spikes that correspond to the total energy of the charge collected in the substrate.

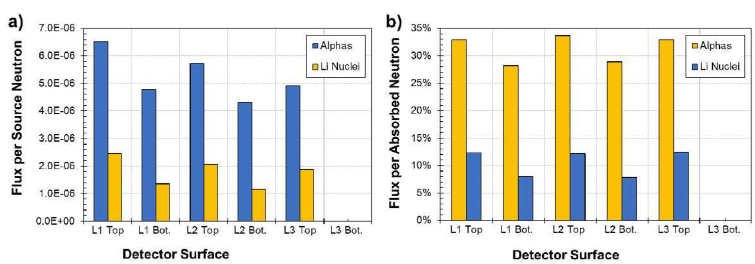

Figure 12. MCNP calculation of fractional flux of alphas and Li nuclei into silicon detector layers from each side of a multilayer device, with a) flux of charged particles per source neutron, and b) flux per absorbed neutron in B/Al converter stack.